Catalysis Today 137 (2008) 379–384

Contents lists available at ScienceDirect

Catalysis Today

journal homepage: www.elsevier.com/locate/cattod

Chlorobenzene total oxidation over palladium supported on ZrO_2, TiO_2 nanostructured supports

J.-M. Giraudon [a,*], T.B. Nguyen [a], G. Leclercq [a], S. Siffert [b], J.-F. Lamonier [b], A. Aboukaïs [b], A. Vantomme [c], B.-L. Su [c]

[a] Unité de Catalyse et Chimie du Solide, UMR CNRS 8181, USTL, Bâtiment C3, 59655 Villeneuve D'Ascq, France
[b] Laboratoire de Catalyse et Environnement, EA 2598, Université du Littoral-Côte d'Opale, 145 Avenue Maurice Schumann, 59140 Dunkerque, France
[c] Laboratoire de Chimie des Matériaux Inorganiques, Université de Namur, Belgium

ARTICLE INFO

Article history:
Available online 16 April 2008

Keywords:
Catalytic chlorobenzene oxidation
Palladium
Porous supports

ABSTRACT

Two series of supported Pd catalysts were synthesized on new mesoporous–macroporous supports (ZrO_2, TiO_2) labelled M (Zr and Ti). The deposition of palladium was carried out by wet impregnation on the calcined TiO_2 and ZrO_2 supports at 400 °C (Pd/Zr_4, Pd/Ti_4) and 600 °C (Pd/Zr_6, Pd/Ti_6) and followed by a calcination at 400 °C for 4 h. The pre-reduced Pd/MX catalysts were investigated for the chlorobenzene total oxidation and their catalytic properties where compared to those of a reference catalyst Pd/Ti-Ref (TiO_2 from Huntsman Tioxide recalcined at 500 °C) and of a palladium supported on the fresh mesoporous–macroporous TiO_2 (Pd/Ti). Based on the activity determined by T_{50}, the Pd/Ti and Pd/Ti_4 catalysts have been found to be more active than the reference one. Moreover activity decreased owing to the sequence: Pd/TiX $\gg$ Pd/ZrX and in each series when the temperature of calcination of the support was raised. The overall results clearly showed that the activity was dependant on the nature of the support. The better activity of Pd/TiX compared to Pd/ZrX was likely due to a better reducibility of the TiO_2 support (Ti^{4+} into Ti^{3+}) leading to an enhancement of the oxygen mobility. Production of polychlorinated benzenes $PhCl_x$ ($x = 2$–6) and of Cl_2 was also observed. Nevertheless at 500 °C the selectivity in HCl was higher than 90% for the best catalysts.

© 2008 Elsevier B.V. All rights reserved.

1. Introduction

Due to their widespread applications in industry, chlorinated volatile organic compounds (chlorinated VOCs) play an important role in air and water pollution. Indeed chlorinated VOCs can be active in the tropospheric ozone formation as well as in the stratospheric ozone depletion. Thus, the abatement of chlorinated compounds in waste gases is highly relevant.

Besides thermal incineration which is the most common method for chlorinated VOCs destruction, catalytic combustion [1] can be a potential alternative when the chlorinated VOCs concentration in the gaseous effluent is low. Indeed rather low operating temperatures (<500 °C) and the possibility to achieve a high efficiency into harmless products such as CO_2, H_2O and HCl makes it rather attractive.

Supported noble metals, especially platinum [2–5] and palladium [6,7] mainly dispersed on alumina can be used for the catalytic combustion of chlorinated aromatics. The intrinsic disadvantage of noble metals is their interaction with Cl leading to polychlorinated by-products ($PhCl_x$) [7]. As it is well known that the nature of the support has great influence on the catalytic properties of the supported palladium catalysts, the effect of the nature of conventional supports was investigated for chlorobenzene total oxidation and it was found that PhCl conversion as well as the congener and isomer distribution differed for various supports [7]. With the aim to better understand the influence of the support on noble metal species new multi-scale pore oxides with high surface as supports were investigated for VOCs abatement [8,9]. In a preliminary study we found that new hierarchically meso-macroporous nanostructured zirconia and titania supported palladium catalysts were active for complete oxidation of chlorobenzene but producing polychlorinated benzenes [9].

In the present work the effect of the calcination temperature of these supports on chlorobenzene conversion and by-products formation of the palladium based catalysts is described in detail. The catalysts have been characterized by S_{BET}, H_2-TPR, XRD, H_2 chemisorption and X-ray photoelectron spectra (XPS) studies. The catalytic performances of these catalysts were compared to those of a Pd catalyst supported on a commercial support, namely TiO_2 supplied by Huntsman Tioxide.

---

* Corresponding author. Tel.: +33 3 20 43 68 56; fax: +33 3 20 43 65 61.
E-mail address: jean-marc.giraudon@univ-lille1.fr (J.-M. Giraudon).

0920-5861/$ – see front matter © 2008 Elsevier B.V. All rights reserved.
doi:10.1016/j.cattod.2008.02.019

2. Experimental

2.1. Preparation of ZrO_2 and TiO_2 oxides and palladium based catalysts

The preparation of the nanostructured TiO_2 and ZrO_2 oxides with hierarchical porosities was achieved according to the procedure given elsewhere [10–12]. The samples were then calcined in dry air at 400 °C and 600 °C for 4 h.

Two series of palladium based catalysts namely titania and zirconia supported palladium catalysts with a loading of 0.5 wt.% were prepared by aqueous impregnating method using palladium nitrate as the metal precursor. The impregnated solids were dried at 100 °C overnight, calcined at 400 °C for 4 h. The final catalysts were designated as Pd/MX, where M stands for Ti or Zr and X is related to the calcination temperature (X = 4 (400 °C); 6 (600 °C)). For comparison, a palladium catalyst loaded on TiO_2 supplied by Tioxide recalcined at 500 °C for 5 h and designed as Pd/Ti-Ref and another on the fresh macroporous–mesoporous titania were prepared in a similar way. The Pd content was measured by atomic absorption at the "Service Central d'Analyses du C.N.R.S." (Vernaison, France) and was found to be close to 0.5 wt.% for all samples.

2.2. Physico-chemical characterization and catalytic test

Phase composition of the samples was determined with a Huber X-ray powder diffractometer with Cu K_α radiation.

The X-ray photoelectron spectra were recorded with a VG ESCALAB 220XL spectrometer (Al K_α = 1486.6 eV). The analyser was operating in a constant pass energy mode (E_{pas} = 40 eV) using the electromagnetic mode for the lens. The Ti $2p_{3/2}$ line was taken as internal reference with a binding energy of 458.5 eV.

Pulse chemisorption measurements were performed using an Altamira AMI-200 apparatus. The samples pre-reduced at 200 °C in a flow of 5% H_2/Ar (30 mL/min) for 2 h were then exposed to a flow of Ar from RT to 400 °C for 2 h before to be cooled down to 100 °C. Pulse chemisorption measurements were performed at that temperature with 5% H_2/Ar.

Hg-porosimetry measurements were performed by "Hg-porosimetry (Caro-Erba 2000). The nitrogen adsorption analysis was performed on Sorptometer 1990 apparatus at −196 °C and the specific surface areas of the catalysts were determined by BET method.

Catalytic activity measurements were carried out in a continuous tubular flow reactor (2 cm o.d.) at atmospheric pressure [9]. The conversion of 1000 ppmv chlorobenzene was investigated in air with a F/w fixed at 220 mln/(min g). The organic reactant and the reaction products were analysed by a VARIAN chromatograph (FID and TCD detectors). HCl and Cl_2 were both trapped at the exit of the reactor in a bubbler containing an aqueous solution of KI (0.1 M). Polychlorinated compounds were identified both by MS (Omnistar) and by GC by the elution of different standards. Aliquot of the bubbler solution was taken at the beginning of each injection. HCl amount was evaluated from $[H_3O^+]$ determined by pH measurement and the amount of chlorine was evaluated from $[I_3^-]$ concentration determined by visible spectroscopy. Conversion was determined from the product distribution in order to avoid errors due to possible variations of the initial flow rate of the VOC during the test.

Conversion was calculated according to:

$$\alpha = \frac{n_{CO_2} + 6n_{PhCl_i}}{n_{CO_2} + 6n_{PhCl_i} + 6n_{PhCl}}$$

The selectivity into HCl was calculated using:

$$S_{HCl} = \frac{n_{HCl}}{n_{HCl} + 2n_{Cl_2} + \sum i \times n_{PhCl_i}} \times 100$$

(n_X: molar quantity of compound X; for n_{PhCl_i}, i stands for the number of chlorine atoms in the polychlororobenzene molecule).

Prior to the catalytic testing each sample was reduced with H_2 at 200 °C (1 °C/min, 2 L/h, 10 h at T_{final}). After cooling down, the catalyst was swept with N_2 (4 L/h) for 0.5 h. The reactor was then heated up to ca. 400 °C (Pd/Zr_4 and Pd/Ti), 500 °C for Pd/Ti_4 and 560 °C for the other ones at a rate of 1 °C/min.

3. Results

3.1. Characterization of the ZrO_2 and TiO_2 oxides and Pd/porous oxides

Surface areas and pores sizes of the fresh and calcined supports are given in Table 1. We notice a decrease of the surface areas when

Table 1
Specific surface area and pore size distribution of oxides before and after calcination at 400 °C and 600 °C

Sample	Untreated		After calcination at 400 °C		After calcination at 600 °C	
	S_{BET} (m^2/g)	Pore size (nm)	S_{BET} (m^2/g)	Pore size (nm)	S_{BET} (m^2/g)	Pore size (nm)
ZrO_2	310	1.2	200	1.2	95	1.8
TiO_2	228	2.9	183	2.9	80	2.6
TiO_2-Ref			210[a]	–		

[a] After calcination at 500 °C.

Table 2
Physico-chemical properties of the fresh and used catalysts

Catalysts	Fresh				After test	
	S_{BET} (m^2/g)	Pore size (nm)	D_{Pd} (%)[a]	d_{Pd} (nm)[b]	S_{BET} (m^2/g)	Cl (wt.%)[c]
Pd/Zr_4	182	1.2	64	1.7	107	1.38
Pd/Zr_6	96	1.8	40	2.8	93	0.44
Pd/Ti_4	188	2.9	50	2.2	108	<0.20
Pd/Ti_6	65	2.6	38	2.9	63	<0.20
Pd/Ti-Ref	177	–	14	8.4	93	0.23

[a] Palladium dispersion.

[b] Mean Pd particle size.

[c] Elemental analysis.

the temperature of calcination is raised while the average pore diameters are practically unchanged. The Ti-Ref support which has been calcined at 500 °C for 4 h has a S_{BET} of 210 m^2/g.

Specific surface areas, Pd dispersions and Pd particle sizes of the catalysts are shown in Table 2. Adding Pd on the support leads to a low decrease of the specific surface area whereas the average pore diameters are unchanged. The specific surface areas of Pd/Zr_4 and Pd/Ti_4 are around two and three times the value for Pd/Zr_6 and Pd/Ti_6, respectively. The Pd dispersion which is 64% (Pd/Ti_4) and 50% (Pd/Zr_4) decreases with the calcination temperature to reach ca. 40% for both samples. It is worth mentioning that the Pd dispersion is rather low on the Pd/Ti-Ref sample (14%). Moreover the mean Pd particle size ranging from 1.7 nm to 2.8 nm for the Zr*X* (*X* = 4–6) supports indicates that most of the Pd particles are likely located at the external surface and into the macropores. By contrast, the Pd mean size of 2.2 nm may allow diffusion of the Pd into the mesopores of Ti_4 whereas it seems to be more difficult for the Pd/Ti_6 sample.

The H_2-TPR profiles of the calcined catalysts are given in Fig. 1. For all catalysts but Pd/Ti-Ref the H_2 consumption is in agreement with the complete reduction of PdO into Pd^0. Hence the TPR runs confirmed that 200 °C, i.e. the temperature used for reduction of the catalysts before kinetic runs, is sufficient for a complete reduction of the palladium oxide.

The Pd $3d_{5/2}$ core level binding energy of about 336.4 (±0.2 eV) for the fresh Pd/Ti*X* agrees with PdO particles dispersed on TiO_2 [13]. It is worth mentioning that the FWHM of the Pd $3d_{5/2}$ signal of Pd/Ti_4 by contrast to the other ones is rather large (2.8 eV) and suggests many defects in the palladium oxide particles. Besides the BE of the O 1s core level of 529.9 eV (±0.2 eV) values for any samples is in agreement with O1s binding energy obtained for the single oxide TiO_2 (Table 5) [14].

3.2. Comparison of the catalytic performances of palladium loaded on various supports

Fig. 2 shows the curves of chlorobenzene conversion in function of the temperature. Conversion of PhCl starts around 150 °C for Pd/Ti*X* samples and 200 °C for the Pd/Zr*X* ones. The 100% chlorobenzene conversion is reached at a temperature of 380 °C (Pd/Ti_4) and of 460 °C (Pd/Zr_6) for the most active catalysts in each series. Based on the T_{50} values (Table 3) one can range the different catalysts by decreasing activity: Pd/Ti_4 (271) > Pd/Ti (276) > Pd/Ti-Ref (296) > Pd/Ti_6 (306) > Pd/Zr_4 (314) > Pd/Zr_6 (346). The Pd/Ti and Pd/Ti_4 catalysts have a similar activity higher than the reference one. Moreover the activity decreases owing to the sequence: Pd/Ti*X* ≫ Pd/Zr*X* and for each series when the calcination temperature of the support is raised. Moreover the dispersion of palladium seems not to be here a crucial parameter. By contrast the overall results clearly showed that the activity was dependent on the nature of the support.

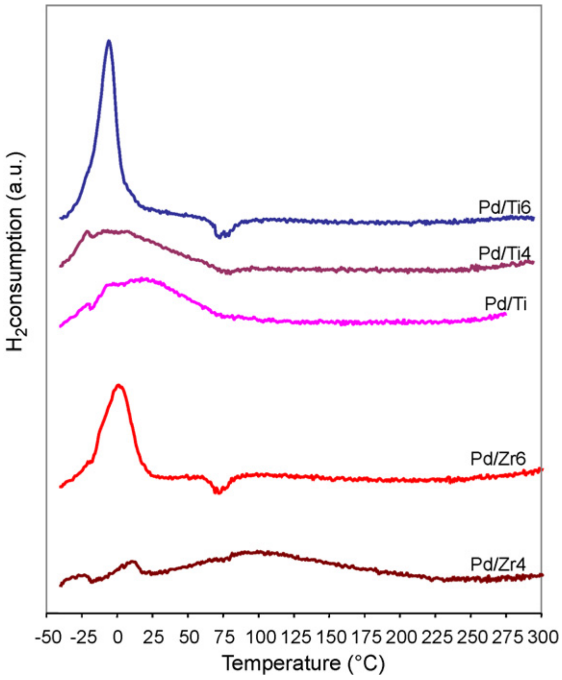

Fig. 1. H_2-TPR of the catalysts.

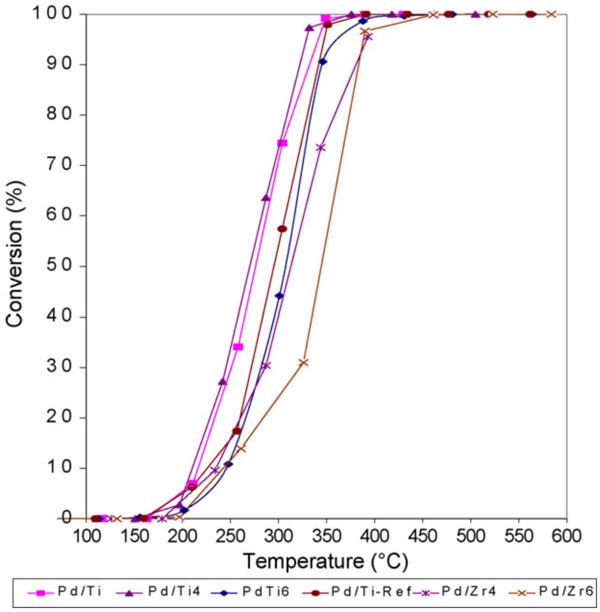

Fig. 2. Chlorobenzene conversion vs. temperature over Pd supported catalysts.

However, the formation of polychlorinated benzenes congeners $PhCl_x$ (x = 2–6) has been observed from 150 °C to 200 °C temperatures on each sample with maxima of production around 300–400 °C. At 350 °C total chlorine production based on polychlorinated benzenes amounts increases as: Pd/Zr_6 < Pd/Zr_4 < Pd/Ti_4 < Pd/Ti < Pd/Ti_6 < Pd/Ti-Ref. Noticeable at 100% chlorobenzene conversion polychlorinated benzenes are always detected on all the catalysts. At 500 °C the $PhCl_x$ production decreases owing to Pd/Ti-Ref > Pd/Ti_6 > Pd/Zr_6 ≫ Pd/Ti_4, no polychlorinated benzenes being observed on Pd/Ti after 450 °C. The amounts of $PhCl_x$ do not appear to correlate with the palladium dispersion and increase with titania based catalysts but all the more the catalyst is active and all the more the temperature of $PhCl_x$ disappearance decreases.

Table 4 shows the concentration of the polychlorinated compounds with the temperature. As the temperature is raised

Table 3
Catalytic properties

Catalyst	T_{final} (°C)	T_{50} (°C)	S_{HCl} at 400 °C	S_{HCl} at 500 °C
Pd/Ti-Ref	565	296	43	68
Pd/Ti	430	276	91	–
Pd/Ti_4	500	271	84	92
Pd/Ti_6	565	306	62	87
Pd/Zr_4	400	314	52[a]	–
Pd/Zr_6	584	346	53	94

[a] At 370 °C.

Table 4
$PhCl_x$ distribution (in ppm $PhCl_x$) over the Pd supported catalysts

Catalysts	T (°C)	1,2-$PhCl_2$	1,3-$PhCl_2$	1,4-$PhCl_2$	1,2,3-$PhCl_3$	1,2,4-$PhCl_3$	1,3,5-$PhCl_3$	1,2,3,4-$PhCl_4$	1,3,4,5-$PhCl_4$	$PhCl_5$	$PhCl_6$
Pd/Ti-Ref	300	13	32	58	9	41	4	28	2	19	2
	400	0	0	0	2	4	0	19	19	32	18
	500	0	0	0	0	0	0	0	14	1	13
Pd/Ti	300	35	29	74	5	34	6	6	4	2	0
	400	0	0	0	0	0	0	3	0	6	4
	500	–	–	–	–	–	–	–	–	–	–
Pd/Ti_4	300	27	33	75	5	43	5	17	4	3	0
	400	0	0	0	0	0	0	5	0	29	8
	500	0	0	0	0	0	0	0	0	0	0
Pd/Ti_6	300	32	42	61	3	32	6	11	5	3	0
	400	1	2	5	4	9	1	34	5	38	9
	500	0	0	0	0	1	0	2	0	6	8
Pd/Zr_4	300	42	18	26	0	10	4	0	0	0	0
	400	–	–	–	–	–	–	–	–	–	–
	500	–	–	–	–	–	–	–	–	–	–
Pd/Zr_6	300	24	16	41	0	3	1	0	0	0	0
	400	0	0	0	2	35	6	28	10	15	1
	500	0	0	0	0	0	0	0	0	2	1

the formation of heavier congeners is observed. The $PhCl_2$ isomers are first produced: 1,2-$PhCl_2$; 1,3-$PhCl_2$ and 1,4-$PhCl_2$. Then the isomers of $PhCl_3$ are detected: 1,2,4-$PhCl_3$; 1,2,3-$PhCl_3$; 1,3,5-$PhCl_3$ with excess of 1,2,4-$PhCl_3$. Then the $PhCl_4$derivatives are observed: 2,3,4-$PhCl_{4,}$ 1,2,4,5-$PhCl_4$ and 1,2,3,5-$PhCl_4$ which have been not separated. Finally $PhCl_5$ and $PhCl_6$ are detected in low amounts. Regarding the mechanism of the chlorination, as stated above, the production of *ortho* and *para* isomers of dichlorobenzene higher than that of the meta isomer strongly suggests an electrophilic substitution on the aromatic ring of hydrogen atom by a chlorine species. The successive electrophilic substitutions also account for the nondetection of 1,2,5-$PhCl_3$ and the presence of 1,2,3,4-$PhCl_4$ as only isomer of tetrachlorobenzene with respect to the Cl *ortho*- and *para*-orientation deactivating Cl substituents. The PdO_xCl_y phase could be responsible for the successive chlorination of chlorobenzene [15]. Indeed due to the electronegativity of oxygen it might be possible that $Cl^{\delta+}$ could exist and be the chlorinating agent. Also Cl_2 is observed in small amounts on each catalyst whose detection begins around 350–450 °C. The high selectivity into HCl of Pd/Ti and Pd/Ti_4 at 400 °C (Table 3) compared to others samples can be explained taking into account that the rates of oxidation of the polychlorinated by-products are presumably higher than their rates of chlorination.

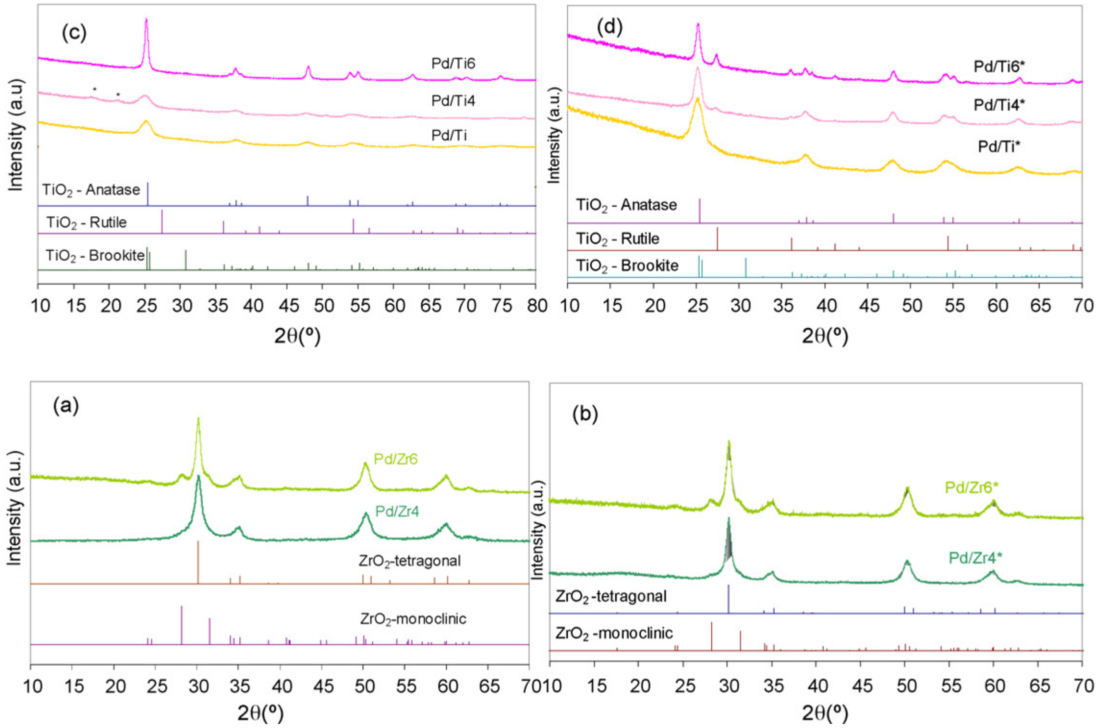

Fig. 3. XRD patterns of the fresh Pd/M*X* samples (a: M = Zr; c: M = Ti) and of the used ones (b: M = Zr; d: M = Ti); (*) lines characteristic of mylar arisen from the experimental preparation of the sample.

Table 5
XPS binding energies (eV) and FWHM (eV) of the fresh Pd/Ti*X* and used Pd/Ti*X** (*X* = 4, 6)

Sample	O 1s		$Pd\ 3d_{5/2}$		Cl 2p	
	BE	FWHM	BE	FWHM	BE	FWHM
Pd/Ti-Ref	529.8	1.8	336.2	2.3	–	–
Pd/Ti-Ref*	529.8	1.6	336.3	3.2	197.6	2.8
Pd/Ti_4	529.8	1.8	336.2	2.8	–	–
Pd/Ti_4*	530.1	1.8	334.4	2.0	n.o.	n.o.
Pd/Ti_6	529.7	1.8	336.2	1.8	–	–
Pd/Ti_6*	530.0	1.8	336.0	2.6	197.9	2.8

Table 6
XPS results on the fresh Pd/Ti*X* and used Pd/Ti*X** catalysts

Summary of XPS (in atomic %) of fresh and spent catalysts						XPS atomic ratios			
Catalyst	Pd	Ti	O	C	Cl	Pd/Ti	O/Ti	Cl/Ti	C/Ti
Pd/Ti-Ref	0.14	31.20	61.15	7.51	–	4.5×10^{-3}	1.97	–	0.24
Pd/Ti-Ref*	0.17	30.03	58.57	10.95	0.28	5.7×10^{-3}	1.95	0.0093	0.36
Pd/Ti_4	0.13	25.39	46.69	27.79	–	5.2×10^{-3}	1.84	–	1.09
Pd/Ti_4*	0.24	25.50	51.75	22.51	–	9.4×10^{-3}	2.02	–	0.88
Pd/Ti_6	0.18	27.71	52.96	19.15	–	6.5×10^{-3}	1.91	–	0.69
Pd/Ti_6*	0.41	25.01	49.67	24.33	0.58	16.3×10^{-3}	1.96	0.023	0.97

3.3. Characterization of the used Pd/porous oxides

The X-ray diffraction patterns of the fresh zirconia supported palladium catalysts do not show Pd related phases owing to its low content. In each pattern the lines characteristic of ZrO_2-tetragonal are observed as well as broad and low intensity lines, assigned to the ZrO_2-monoclinic phase, which appear better resolved and whose relative intensities slightly increase as the temperature of calcination is raised. This clearly indicates that the crystallization process of each phase goes deeper and also suggests that ZrO_2-tetragonal partially transforms into ZrO_2-monoclinic as the temperature is raised. Regarding the titania supported palladium catalysts, all XRD patterns show only the lines ascribed to the TiO_2-anatase phase which sharpen when the temperature of calcination increases indicating again a better crystallization of the support.

The XRD patterns of the used Pd/Zr*X* do not show significant modifications compared to those before testing (Fig. 3a and b). On the contrary on the X-ray diffractions patterns of the used nanostructured porous titania catalysts (compare Fig. 3c and d) it was observed that TiO_2 undergoes partially anatase to rutile phase transition, whereas no such a phase transition was observed for the Pd/Ti-Ref. Furthermore the relative intensity of the rutile phase significantly increases with the calcination temperature. There is also a significant decrease of the specific surface areas for all samples whose supports have been stabilized at 400 °C contrarily to the ones calcined at 600 °C which are rather stable (Table 2).

The Pd/Ti-Ref, Pd/Ti_4 and Pd/Ti_6 have been characterized by XPS after test and the results are listed in Tables 5 and 6. Decomposition of the $Pd\ 3d_{5/2}$ spectra shows two components: one at 335.1 eV and the other at 336.8 (±0.3 eV) indicative of Pd° and Pd^{2+}. The atomic percentage of metallic palladium decreases owing to: Pd/Ti_4 (80%) > Pd/Ti-Ref (41%) > Pd/Ti_6 (31%). Regarding the palladium dispersion which is of 50%, 14% and 38%, Pd/Ti_4 which is the most dispersed catalyst for which the contact between oxygen and palladium is favoured would be expected to be more oxidized. This can be explained since the final temperature of the test T_f is ca. 60 °C lower for Pd/Ti_4 compared to the others ones. It must be suggested that the fraction of palladium zero is important at low temperatures on the catalysts. It must be added that the XPS Pd/Ti ratios show a significant palladium enrichment at the surface of the titania porous catalysts contrarily to Pd/Ti-Ref. Moreover chlorine was undetected at the surface of Pd/Ti_4 contrarily to Pd/Ti_6 and Pd/Ti-Ref. The binding energy values of Cl $2p_{3/2}$ at 197.7 (±0.2 eV) on the two samples are consistent with inorganic chlorine entities. Chlorine retention has also been determined by elemental analysis (Table 2) and decreases owing to: Pd/Zr*X* ≫ Pd/Ti*X*. The higher chorine value obtained on Pd/Zr_4 whose final temperature of catalytic testing is 400 °C compared to the one of 0.44 for Pd/Zr_6 suggests a higher retention of chlorine on the catalyst at low temperature which desorbs mainly as HCl as the temperature is raised.

4. Discussion

As previously mentioned the better activity of the Pd/TiO_2 samples compared to the Pd/ZrO_2 ones does not depend upon the palladium dispersion, reducibility of PdO or specific surface area. As it is well known that TiO_2 is more reducible than ZrO_2, the better reducibility of the TiO_2 support (Ti^{4+} into Ti^{3+}) can lead to an enhancement of the oxygen mobility by the creation of oxygen vacancies.

We propose here a reaction scheme previously proposed for palladium supported on perovskite having mobile oxygen [16].

- In the first step the $Ti^{4+}O_x$ species supply oxygen species from the network to oxidize chlorobenzene and are transformed into $Ti^{3+}O_y$ species.
- In the second step the $Ti^{3+}O_y$ species are reoxidized by dioxygen which has been supposed to be previously dissociated on palladium sites.

The following scheme is the following:

$$VOC + * \leftrightarrows VOC_{ads}$$

$$O_2 + 2* \leftrightarrows 2O_{ads}$$

$$VOC_{ads} + \ll O \gg \rightarrow VOC_{ox} + \text{«}\square\text{»}$$

$$\text{«}\square\text{»} + O* \leftrightarrows \ll O \gg$$

where * is a free site of palladium, «O» is the active oxygen, VOC_{ox} is the organic molecule partially oxidized and «□» an oxygen vacancy. The activities of the catalysts seem here to be related to the availability of oxygen species in the initial solid, in accordance with the hypotheses put above on the mechanism scheme of the reaction since the refilling of the oxygen vacancies must be rapid due to the catalytic effect of palladium. This can explained why the catalysts whose the support has been calcined at lower temperatures are more active.

5. Conclusion

A new generation of supported on porous zirconia, titania palladium catalysts were synthesized. The supports were stabilized at 400 °C and 600 °C. The catalysts on mesoporous–macroporous titania exhibit higher catalytic activity than the zirconia supported palladium catalysts. The better activity of Pd/TiO_2 compared to Pd/ZrO_2 was likely due to a better reducibility of the TiO_2 support (Ti^{4+} into Ti^{3+}) indicating an enhancement of the oxygen mobility. The activity seems to be dependent on the availability of mobile oxygen which is related to the calcination temperature of the support.

A production of significant amounts of polychlorinated benzenes $PhCl_x$ ($x = 2–6$) is observed on all catalysts. Chlorination of the aromatic ring on PdO_xCl_y related phases via a mechanism of successive electrophilic substitution reactions may account for the distribution of the different isomers of the congeners $PhCl_x$. The temperature of polychlorinated benzenes disappearance decreases all the more than the catalyst is active.

Acknowledgements

The authors thank the European community through an Interreg IIIa France-Wallonie-Flandre project and Walloon Region for financial supports.

References

[1] G.C. Bond, N. Sadeghi, J. Appl. Chem. Biotechnol. 25 (1975) 241.
[2] D.M. Papenheier, J.A. Rossin, Ind. Eng. Chem. Res. 33 (1994) 3094.
[3] J.A. Rossin, M.M. Farris, Ind. Eng. Chem. Res. 32 (1993) 1024.
[4] H. Windawi, Z.C. Zhang, Catal. Today 30 (1996) 99.
[5] R.W. van den Brink, R. Louw, P. Mulder, Appl. Catal. B 16 (1998) 219.
[6] L. Becker, H. Forster, J. Catal. 170 (1997) 200.
[7] R.W. van den Brink, M. Krzan, M.M.R. Feijen-Jeurissen, R. Louw, P. Mulder, Appl. Catal. B 24 (2000) 255.
[8] V. Idakiev, L. Ilieva, D. Andreeva, J.L. Blin, L. Gigot, B.-L. Su, Appl. Catal. A 243 (2003) 25.
[9] H.L. Tidahy, S. Siffert, J.-F. Lamonier, E.A. Zhilinskaya, A. Aboukaïs, Z.-Y. Yuan, A. Vantomme, B.-L. Su, X. Canet, G. de Weireld, M. Frère, T.B. Nguyen, J.-M. Giraudon, G. Leclercq, Appl. Catal. A 310 (2006) 61.
[10] Z.Y. Yuang, T.Z. ren, A. Vantomme, B.-L. Su, Chem. Mater. 16 (2004) 5096.
[11] J.–L. Blin, A. Léonard, Z.-Y. Yuang, L. Gigot, A. Vantomme, A.K. Cheetham, B.-L. Su, Angew, Chem. Int. Ed. 42 (2003) 2872.
[12] Z.-Y. Yuang, A. Vantomme, A. Léonard, B.-L. Su, Chem. Commun. (2003) 1962.
[13] National Institute of Standard and Technology, NIST X-ray photoelectron spectroscopy database, http://srdata.nist.gov/xps/.
[14] R. Castillo, B. Koch, P. Ruiz, B. Delmon, J. Catal. 161 (1996) 524.
[15] M. Taralunga, J. Mijoin, P. Magnoux, Catal. Commun. 7 (2006) 115.
[16] A. Elhachimi, PHD Thesis, Lille 2005.